Intergrain exchange coupling and coercivity mechanism of nanocrystalline $Sm_2Fe_{15-x}Cu_xSi_2C$ ($x=0$ and 1) ribbons prepared by melt spinning

Hong-wei Zhang, Zhi-gang Sun, Shao-ying Zhang, Bao-shan Han, and Bao-gen Shen
State Key Laboratory of Magnetism, Institute of Physics and Centre for Condensed Matter Physics, Chinese Academy of Sciences, Beijing 100080, China

I-Chung Tung and Tsung-Shune Chin
Department of Materials Science and Engineering, National Tsing Hua University, Hsinchu 30043, Taiwan, Republic of China
(Received 21 December 1998)

Transmission electron microscopy (TEM), high resolution transmission electron microscopy (HRTEM), and magnetic force microscopy (MFM) have been employed to image the microstructure and magnetic domain in nanocrystalline melt-spun $Sm_2Fe_{15-x}Cu_xSi_2C$ ($x=0$ and 1) ribbons. Due to the unnegligible intergrain exchange coupling, the diminution of magnetic surface charges and the enhancement of remanence are observed in $Sm_2Fe_{15}Si_2C$ ribbons, while the intergrain exchange coupling is suppressed by the presence of mainly Cu contained grain boundary. The revision of coercivity mechanism in modified Brown's expression is discussed as the grain size in nanoscale regime. [S0163-1829(99)08425-8]

I. INTRODUCTION

A new dimension has been added to magnetic intermetallics by interstitial modification. The effects of interstitial modification are dramatic, particularly on the Curie temperature and magnetocrystalline anisotropy of iron-based intermetallics, such as nitrides or carbides of Sm_2Fe_{17}, making them suitable candidates for permanent magnets.[1,2] As the substitution of Fe with an element such as Ga, Al, Si, or Cr can stabilize the high carbon content R_2Fe_{17} carbides up to high temperature,[3–7] high coercivity has been obtained in $Sm_2(Fe,M)_{17}C_x$ ($M=$Ga, Al, Si, and Cr) by melt-pinning or mechanical alloying techniques[7–13] other than by the low-temperature gas-phase interstitial modification.

Our previously studies have shown that small Cu additions are very effective in enhancing the coercivity of melt-spun $Sm_2(Fe,M)_{17}C_x$ ($M=$Si or Ga) ribbons.[13,14] However, the role of additive Cu is not well understood. In isotropic ribbons, the remanence is half of the saturation M_s predicted by Stoner-Wohlfarth model. The remanence enhancement has been observed where the value of the reduced remanence $m_r=M_r/M_s=0.6$ is larger than 0.5 for $Sm_2Fe_{15}Si_2C$ ribbons, while the value of m_r is about 0.48 for $Sm_2Fe_{14}CuSi_2C$ ribbons. The remanence enhancement was conceptually explained resulting from significant ferromagnetic exchange coupling between the nanoscale grains by Kneller and Hawig,[15] which is further more demonstrated by computational micromagnetism.[16–18] But the effect of intergrain exchange coupling on magnetic domain and demagnetization process is not well investigated experimentally.

In this paper, the intergrain exchange coupling and coercivity in nanocrystalline melt-spun $Sm_2Fe_{15-x}Cu_xSi_2C$ ribbons will be reported.

II. EXPERIMENTS

The ingots with nominal compositions of $Sm_2Fe_{15-x}Cu_xSi_2C$ ($x=0$ and 1) were prepared by arc-melting the constituent materials Sm, Fe, Cu, and Si (with a purity of at least 99.9%) and Fe-C alloy (5.2 wt. % C) under high purified argon atmosphere. The ribbons were obtained using a melt-spinning technique. The surface velocity of the Cu wheel was 20 m/s for $x=0$ (Cu-free) and 15 m/s for $x=1$ (Cu-doped), respectively. X-ray diffraction patterns indicated that the ribbons mainly consist of a single Th_2Zn_{17}-type structure phase. Microstructure was observed by transmission electron microscopy (TEM), and a closer investigation of grain boundary of the matrix phase in the ribbons has been undertaken with high resolution transmission electron microscopy (HRTEM). The energy dispersive x-ray (EDX) analysis was used to determine the chemical contents of the elements. Atomic force micrograph (AFM) and magnetic force microscopy (MFM) images were obtained using a Digital Instruments Nanoscope IIIA multimode scanning probe microscope under a scanning mode described by the Digital Instruments as Interleave Scanning with Lift Mode. The scan height is 30 nm.

III. RESULTS AND DISCUSSION

The representative micrographs measured by TEM are shown in Fig. 1. Both average grain sizes of Cu-free and Cu-doped ribbons are samely about 60 nm. These grain sizes is smaller than the single domain size of Sm_2Fe_{17} nitrides. The distributions of grain size of both samples are not brightly different.

Figure 2 shows the micrograph examined by HRTEM of Cu-doped samples. About 2 nm width grain boundary can be found between two matrix 2:17 phase grains. The average atomic ratios of Sm:Fe:Si:Cu obtained by EDX were 10.4:72.9:12.5:4.2 and 18.5:25.0:7.0:49.5 for the matrix phase and the grain boundary of Cu-doped samples, respectively. It can be concluded that addition element Cu mainly gathers inter-grain and forms Cu-rich grain boundary.

Figures 3(a) and 3(b) show AFM (left) and MFM (right) images with a scan size 5 μm$\times$5 μm from the Cu-doped

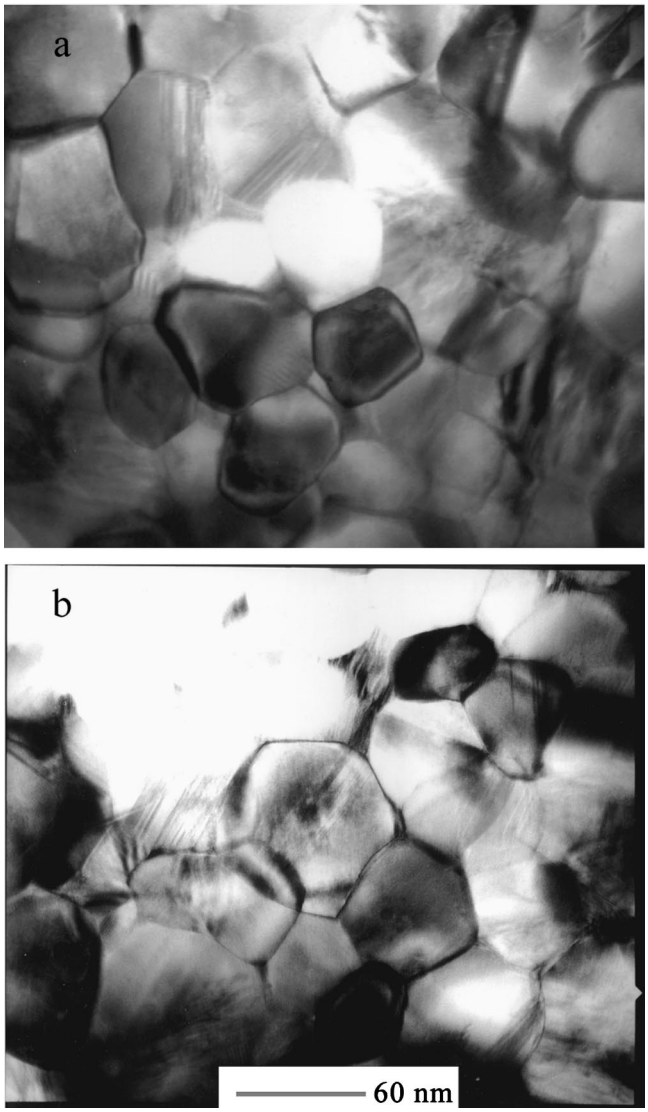

FIG. 1. The representative micrographs of Cu-free (a) and Cu-doped (b) ribbons measured by TEM.

and Cu-free samples in frequency mode, respectively. Magnetic imaging was undertaken using high coercivity magnetic sputter coated probes (Co-Cr coated), magnetized in a direction perpendicular to the sample surface. The probe acts as a fixed dipole when imaging, and variation of sample magnetization map to light and dark contrast areas. The magnetic image exhibits the existence of large interaction domains ranging over 300–500 nm for Cu-doped and slightly larger for Cu-free sample, which implies that at least several tens of grains align their magnetization at almost most direction. We can ensure from the picture that the topography has no significant effect on the MFM image. Previous investigation of domain structures of nanocrystalline NdFeB/Fe_3B systems demonstrated the existence of interaction domains (uniformly magnetized regions extending over several crystallites).[19,20] The magnetic domain sizes are several times larger than the grains size of both Cu-doped and Cu-free samples, respectively. The black/white signal reversal, which is sensitive to magnetic surface charges density, is much stronger in Cu-doped MFM image than in Cu-free MFM image. In a boundary region between two neighboring

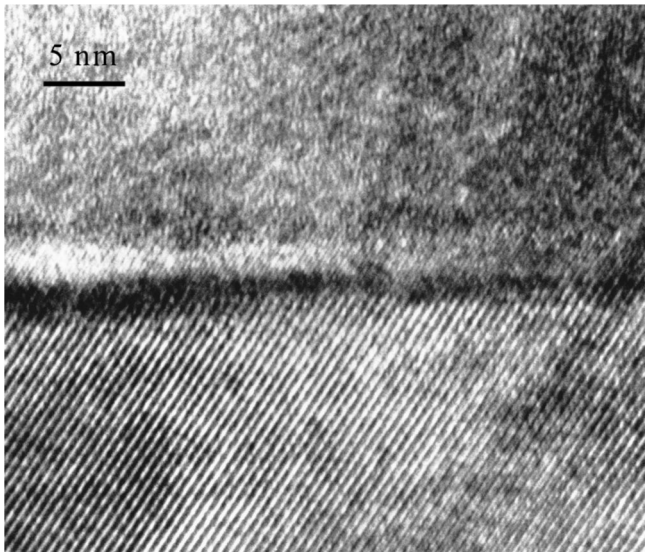

FIG. 2. The micrograph examined by HRTEM of Cu-doped samples.

grains, the exchange coupling is acting in addition to the anisotropy, leading to a smooth rotation of the magnetization vector from the easy-axis orientation in one grain to that of the other. Intergrain exchange coupling can decrease the magnetic surface charge density of the ribbons. So, it can be explained that intergrain exchange coupling is much stronger in Cu-free ribbons than that in Cu-doped ribbons. The intergrain exchange coupling has been suppressed by the nonmagnetic mainly Cu-composed grain boundary for Cu-doped ribbons.

Simultaneously, it is due to the existence of Cu-rich grain boundary that the reduced remanence $m_r = 0.48$ for Cu-doped ribbons is nearly the same as the theoretical limit

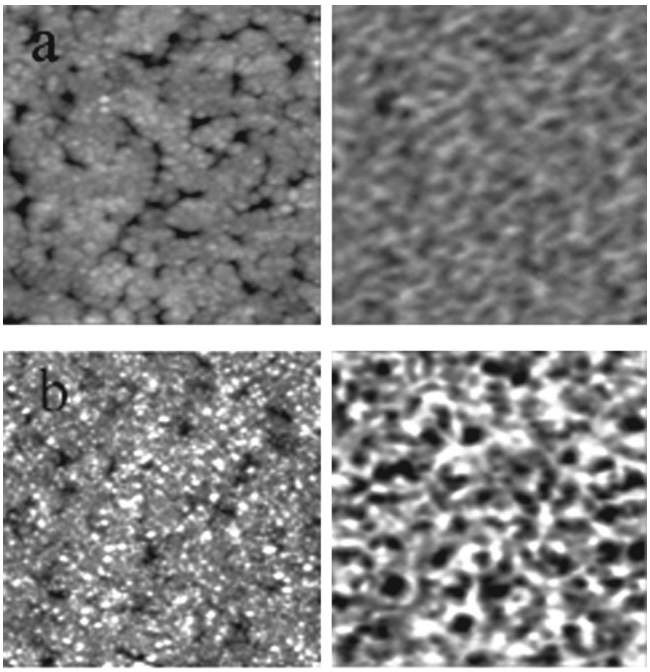

FIG. 3. The AFM (left) and MFM (right) images with a scan size 5 μm$\times$5 μm for the Cu-free (a) and Cu-doped (b) samples in frequency mode.

TABLE I. Our previous results of m_r, ${}_iH_c$, α_k, and N_{eff} about Cu-free and Cu-doped ribbons in new forms (Ref. 13).

Ribbons	m_r	${}_iH_c$ (kOe)	α_k	N_{eff}
Cu-free	0.60	8.4	0.40	0.93
Cu-doped	0.48	13.2	0.72	1.88

value 0.5 of isotropy isolated grains assemble system. On the contrary, $m_r(=0.60)$ being larger than 0.5 for Cu-free ribbons is due to the nonexistence of nonmagnetic grain boundary. Table I lists our previous results about Cu-free and Cu-doped ribbons in new forms.[13] The intrinsic coercivity was analyzed according to well-known modified Brown's formula:[21,22]

$$ {}_iH_c = 2\alpha_k\alpha_\varphi K/\mu_0 M_s - N_{\text{eff}} M_s , \tag{1}$$

where α_k depends on the nature and size of the defect regions in which nucleation or pinning takes place, and α_φ takes account of the misalignment of the grains in the magnet, N_{eff} is the averaged local effective demagnetization factor.

Both the α_k and N_{eff} of Cu-doped samples are about twice times larger than the corresponding ones of the Cu-free samples. The traditional explanation is that the large local demagnetizing factors, helping to invert the magnetization and reducing ${}_iH_c$, can be expected near the nonmagnetic inclusions and sharp edges of the grains, and the small value of α_k indicates that the inhomogeneous layer on the grain surface of sample is thick. It is of interest to note that in Cu-doped ribbon, $\alpha_k = 0.72$ (nearly 1) indicates rather perfect grain surfaces. It is seemingly not reasonable to view that the difference between microstructure factors can be mainly resulted from two nearly same microstructures (as shown in Fig. 1) except for the existence of the grain boundary mainly composed of nonmagnetic Cu in Cu-doped samples (as shown in Fig. 2). As discussed above, the difference between those microstructures factor may be at least partially concerned with the intergrain exchange coupling.

The total energy is the sum of the magnetocrystalline anisotropy energy F_K, the Zeeman energy F_H, the long-range stray field energy F_S and the short-range exchange energy F_{ex}. As the size of the crystallites decreases no more than single domain and the crystallites are not surrounded or separated from each other by nonmagnetic layer, the exchange energy with neighboring crystallites may no longer be negligible compared to the anisotropy energy. However, only the dominant deteriorating microstructures with the regions of reduced magnetocrystalline anisotropy, misaligned grains and the stray field were concerned in the modified Brown's expression.

Intergrain exchange coupling forces magnetization to deviate somewhat from the local easy axis, leading to anisotropy and demagnetization field diminution and remanence enhancement in Cu-free sample. Now, we try to give a new form according to Eq. (1) as follows:

$$ {}_iH_c = \frac{2\alpha_k\alpha_\varphi}{1+6\beta_k l_{\text{ex}}/d} K/\mu_0 M_s - \frac{N_{\text{eff}}}{1+6\beta_s l_{\text{ex}}/d} M_s , \tag{2}$$

where l_{ex} is the ferromagnetic exchange length, d is the grain size, β_k and β_s depend on the nature of the grains boundary concerning anisotropy field and stray field, respectively. Here, we prefer to choose $(A/\mu_0 M_s^2)^{1/2}$,[23] rather than $(A/K)^{1/2}$ as the expression of the exchange length, just because the anisotropy has been taken into consideration in the first term of Eq. (1). Both the values of β_k and β_s are less than 1.

When $d > l_{\text{ex}}$, the term of $6l_{\text{ex}}/d$ is approximated from the reduced exchanging volume $v \propto [(d/2)^3 - (d/2 - l_{\text{ex}})^3]/(d/2)^3 = 6l_{\text{ex}}/d - 3(2l_{\text{ex}}/d)^2 + (2l_{\text{ex}}/d)^3$. As $6l_{\text{ex}}/d \ll 1$, the equation (2) can be expressed in the form of Eq. (1).

For Cu-doped ribbons, the values of β_k and β_s are reasonably considered as far less than 1 approximately. Compared with Cu-doped ribbons, both the value of β_k and β_s in Cu-free ribbons can be regarded as 1, which means intergrain exchange coupling takes place completely, because the reduced remanence we obtained is in compliance with theoretical calculating result 0.6 given in literature.[18] Then Eq. (2) can be changed to the following expression:

$$ {}_iH_c = \frac{2\alpha_k\alpha_\varphi K/\mu_0 M_s - N_{\text{eff}} M_s}{1+6\beta l_{\text{ex}}/d}, \tag{3}$$

where $\beta = \beta_k = \beta_s = 1$.

As the values of average single domain size being 400 nm (as shown in Fig. 3), the factor of exchange coupling A is about 8×10^{-12} J/m according to $d_c = 72(AK)^{1/2}/\mu_0 M_s$. In the case of $d = 60$ nm and the expression of $l_{\text{ex}} = (A/\mu_0 M_s^2)^{1/2} \approx 3.0$ nm, $6l_{\text{ex}}/d$ is nearly 0.30, then $1/(1 + 6l_{\text{ex}}/d) \approx 0.77$. So the real value of α_k and N_{eff} in our new expressions of Cu-free ribbons are 0.55 and 1.45, respectively. Additive Cu makes the value of α_k and N_{eff} increase to 0.72 and 1.88 from 0.55 and 1.45, respectively. The detailed investigation will be given further.

ACKNOWLEDGMENT

This work was supported by the State Key Program of Basic Research, National Science Foundation of China.

[1] J.M.D. Coey and H. Sun, J. Magn. Magn. Mater. **87**, L251 (1990).

[2] X.P. Zhong, R.J. Radwanski, F.R. de Boer, T.H. Jacobs, and K.H.J. Buschow, J. Magn. Magn. Mater. **86**, 333 (1990).

[3] B.G. Shen, L.S. Kong, F.W. Wang, and L. Cao, Appl. Phys. Lett. **63**, 2288 (1993).

[4] B.G. Shen, F.W. Wang, L.S. Kong, L. Cao, and W.S. Zhan, J. Appl. Phys. **75**, 6253 (1994).

[5] Z.H. Cheng, B.G. Shen, F.W. Wang, J.X. Zhang, H.Y. Gong, and J.G. Zhao, J. Phys.: Condens. Matter **6**, L185 (1994).

[6] G.C. Hadjipanayis, Y.H. Zheng, A.S. Murthy, W. Gong, and F.M. Yang, J. Alloys Compd. **222**, 49 (1995).

[7] Zhongmin Chen and G.C. Hadjipanayis, J. Magn. Magn. Mater. **171**, 261 (1997).
[8] J. van Lier, M. Seeger, and H. Kronmuller, J. Magn. Magn. Mater. **167**, 43 (1997).
[9] L. Cao, A. Handstein, W. Grunberger, J. Edelman, L. Schultz, and K.-H. Muller, Appl. Phys. Lett. **68**, 129 (1996).
[10] L.S. Kong, B.G. Shen, F.W. Wang, L. Cao, H.Q. Guo, and T.S. Ning, J. Appl. Phys. **75**, 6250 (1994).
[11] J.X. Zhang, Z.H. Cheng, and B.G. Shen, J. Appl. Phys. **79**, 5528 (1996).
[12] H.W. Zhang, S.Y. Zhang, B.G. Shen, and L.G. Zhang, J. Phys. D **30**, 3085 (1997).
[13] H.W. Zhang, S.Y. Zhang, B.G. Shen, and L.G. Zhang, J. Appl. Phys. **83**, 4838 (1998).
[14] S. Y. Zhang, H. W. Zhang, B. G. Shen, and T. S. Chin, J. Phys. D **31**, 3337 (1998).
[15] Eckart F. Kneller and Reinhard Hawig, IEEE Trans. Magn. **27**, 3588 (1991).
[16] R. Fischer, T. Leineweber, and H. Kronmuller, Phys. Rev. B **57**, 10 723 (1998).
[17] H.M. Jin, Y.B. Kim, and X.F. Wang, J. Phys.: Condens. Matter **10**, 7243 (1998).
[18] V. Neu, A. Hubert, and L. Schultz, J. Magn. Magn. Mater. **189**, 391 (1998).
[19] M. Gibbs, M. Al-Khafaji, W. Rainforth, H. Davies, K. Babcock, J. Chapman, and J. Heyderman, IEEE Trans. Magn. **31**, 3349 (1995).
[20] L. Folks, R.C. Woodward, K.L. Babcock, D.L. Bradbury, K. Humphrey, and R. Street (unpublished).
[21] W.F. Brown, Rev. Mod. Phys. **17**, 15 (1945).
[22] H. Kronmuller, Phys. Status Solidi B **144**, 385 (1987).
[23] K. O'Donnell and J.M.D. Coey, J. Appl. Phys. **81**, 6310 (1997).